Broad Iron Lines in Active Galactic Nuclei

J. Wilms[1] [*], E. Kendziorra[1] and C. S. Reynolds[2]

[1] Institut für Astronomie und Astrophysik, Abt. Astronomie, Sand 1, 72076 Tübingen,
  Germany
[2] Department of Astronomy, University of Maryland, College Park, MD 20742, USA

Abstract The Fe Kα lines seen in many Active Galactic Nuclei (AGN) are thought
to originate close to the central supermassive black hole. In this review we summarize the physics of the fluorescent line formation and show that Fe Kα line profile
observations can be used to probe relativistic effects in the vicinity of the black
hole, concentrating on recent results from *XMM-Newton*.

Key words: accretion, accretion physics — black hole physics

1 INTRODUCTION

The study of relativistically broadened fluorescent iron Kα lines in the spectra of Active Galactic
Nuclei (AGN) presents one of the few possibilities to gain insight into the behavior of material in the strong gravitational field close to supermassive black holes. Starting with an introduction into the physics of relativistic broadening (Sect. 2), in this contribution we review
recent observational results from the *XMM-Newton* observatory. We concentrate on the case of
MCG−6-30-15, with its well studied example of an extremely broadened Fe Kα line (Sect. 3).
Finally, Sect. 4 summarizes our main points, extends the discussion to other AGN apart from
MCG−6-30-15, and gives a short outlook to possible future observations. Due to the limited
space available we will concentrate on the key issues here and refer to the recent exhaustive
reviews of Reynolds & Nowak (2003) and Fabian et al. (2000) for more detailed information.
We will also concentrate on relativistic lines from AGN, although most of the arguments given
below also apply to relativistic lines from Galactic black hole candidates, as observed, e.g.,
in GX 339−4 (Nowak et al., 2002), XTE J1650−500 (Miller et al., 2002), or GRS 1915+105
(Martocchia et al., 2002).

2 RELATIVISTICALLY BROADENED FE Kα LINES

2.1 Continuum Formation in AGN and Galactic Black Holes

There is now general consensus that the X-rays observed from AGN are formed close to the
central supermassive black hole. Current thought is that the observed X-ray power law continuum is formed by the Comptonization of soft photons from a geometrically thin, optically

[*] E-mail: `wilms@astro.uni-tuebingen.de`
Present address: Department of Physics, University of Warwick, Coventry, CV4 7AL, U.K.

thick accretion disk in a hot and possibly extended electron plasma, the "accretion disk corona" (ADC), with an electron temperature $kT_e > 100\,\text{keV}$ (see, e.g., Haardt, 1997, for a review). Due to the similar properties of AGN and of Galactic black hole candidates (BHC), there is also general agreement that the physical processes at work in these two classes of objects are similar.

For both kinds of systems, BHCs and AGN, the relative geometry of the accretion disk and the ADC is still debated. Compton cooling arguments rule out an ADC that fully covers both sides of the accretion disk (Dove et al., 1997), as the high temperatures needed by the 100 keV spectral cutoff cannot be sustained in this "sandwich geometry". It has been proposed, therefore, that sandwiching ADC only partly cover the accretion disk (e.g., Stern et al., 1995; Haardt et al., 1994), or, alternatively, that the ADC and the accretion disk are physically separated. Examples for the latter case are the "sphere and disk" like geometries that have been used successfully to describe the X-ray spectra of Galactic BHC and (e.g., Nowak et al., 2002; Zdziarski et al., 1998; Dove et al., 1997). Here the ADC is represented by an inner, geometrically thick accretion flow, which is surrounded by the geometrically thin standard accretion disk. These "sphere and disk" geometries also seem to be able to reproduce several correlations found between the spectral parameters of AGN (e.g., Zdziarski et al., 1999).

While most work in the past years has been mainly concentrated on the relationship between the ADC and the accretion disk, we note that in recent years it has been realized that weak collimated outflows of (possibly relativistic) particles might be a further necessary ingredient to the models for the creation of the X-ray spectrum, even in the radio-quiet Seyfert galaxies, either through the contribution of synchrotron radiation, or through a synchrotron self-Compton (SSC) component. These models were first suggested for the case of Galactic BHC (Markoff et al., 2001, 2003; Fender, 2001, and references therein), and have recently also been applied to Seyfert galaxies (Ghisellini et al., 2004). While these models are very interesting, the available space prohibits their further discussion.

2.2 Compton Reflection in AGN

Common to all physical processes responsible for the generation of the X-ray continuum is the postulate that primary ("seed") photons are Compton upscattered in the ADC. A trivial consequence of the scattering process is that the direction of the Compton upscattered photons is changed. This means that part of the upscattered hard radiation is intercepted by the comparably cold material of the accretion disk. Owing to the E^{-3}-proportionality of the photoabsorption cross section, photons from the ADC with energies $\gg 10\,\text{keV}$ will mainly interact with the accretion disk through Thomson scattering off the (bound) electrons of the disk material. Since the relative energy change per Thomson scatter is $\Delta E/E \sim -E/m_e c^2$, these photons are typically downscattered in energy. For photon energies $\ll 10\,\text{keV}$, photoabsorption is the dominant mechanism of interaction. The result of the interplay between Thomson scattering at high and photoabsorption at low energies is the formation of a "Compton reflection hump", with a peak flux at $\sim 30\,\text{keV}$ (Lightman & White, 1988; White et al., 1988; Magdziarz & Zdziarski, 1995). The absorption of photons in the inner shell of atoms in the accretion disk also leads to fluorescent line emission from transitions of outer shell electrons to the inner shell vacancy caused by the photoabsorption. As a result of its large cosmic abundance and its large fluorescence yield, lines from iron, especially Fe Kα at 6.4 keV, are by far the strongest fluorescent lines predicted (Basko, 1978; Lightman & White, 1988; Fabian et al., 1989).

The picture outlined above predicts that the observed X-ray spectrum of AGN and Galactic BHC above about 2 keV consists of a power-law continuum due to Comptonization (and possibly also a SSC contribution), the Compton reflection hump, seen as a steepening above $\sim 10\,\text{keV}$ and a peak at 30 keV, and fluorescent line emission, most easily detectable at 6.4 keV. The predicted strength of the latter two reprocessing features depends on the closeness of the source

of the hard photons and the reprocessing material. Due to its model dependence, this closeness is generally expressed in terms of the covering factor $\Omega/2\pi$ of the cold material as seen from the source of hard photons, when modeling data with theoretical models.

2.3 Relativistic Effects

So far, our discussion has concentrated on the physics as it is happening in the frame of rest of the emitting material. For observers distant from the X-ray source, we also have to take into account the observational effects imposed on the radiation on its way from the site of emission to the X-ray telescope. For radiation emitted from a (supposedly Keplerian) accretion disk in the vicinity of a supermassive black hole, the most important effects to be considered are the Doppler shift caused by the relativistic speed of the emitting material, the effect of gravitational light bending, and the gravitational redshift. In the following we give a quantitative description of the major effects, see the reviews mentioned above as well as the specialized literature for the results of numerical computations (e.g., Cunningham, 1975; Fabian et al., 1989; Laor, 1991; Speith et al., 1995; Bromley et al., 1997; Martocchia et al., 2002). Since all of the relativistic effects depend on the location from where the line is emitted, the final ingredient needed for predicting theoretical line profiles is the Fe Kα emissivity per comoving area element of the disk, $\epsilon(r)$, which typically depends on the distance r from the black hole. The final line profile is then obtained by integrating over the contributions from the different disk annuli. In the following illustration of the physics of relativistic broadening, we will first assume $\epsilon(r) \propto r^{-3}$, before then discussing the effect of more general emissivity profiles.

Only a small fraction of the line emitting material from a Keplerian accretion disk is seen to be at rest relative to distant observers, while most material is either seen to be receding or moving towards the observers. As a result, emission lines from accretion disks are expected to exhibit a double humped line profile (Frank et al., 1992). Since the line of sight velocity is $v_\parallel = v \sin i$, where i is the inclination of the disk, these profiles broaden as the disk is seen more edge on at larger inclinations. The left panel of Fig. 1 illustrates this effect for a Keplerian accretion disk around a Schwarzschild BH. Since the speed at the innermost stable circular orbit in these disks is $v \sim 0.3c$, relativistic beaming results in the blue wing of the line to have a larger intensity than the red wing. Furthermore, the line profile is also slightly redshifted because of the gravitational redshift caused by the supermassive black hole. As shown in Fig. 1, the gravitational redshift dominates for low inclinations, where we assumed a realistic Fe Kα emissivity per unit comoving area of the disk of $I_{K\alpha} \propto r^{-3}$. We will discuss the effects of varying this emissivity profile below.

Close to the black hole, the structure of the accretion disk is dominated by the angular momentum of the black hole, which we will characterize by its canonical angular momentum $a = J/Mc$, where $|a| < 1$, and where $a > 0$ implies that the accretion disk and the black hole are corotating (Thorne, 1974). For the most simple accretion disk models of the Shakura & Sunyaev (1973) type, it is assumed that they have a (pseudo-)Keplerian velocity profile down to the marginally stable orbit, r_{ms}, from where on the material falls into the black hole (the "plunging region"). For a non-rotating Schwarzschild black hole, $r_{\mathrm{ms}} = 6r_{\mathrm{g}}$, where $r_{\mathrm{g}} = GM/c^2$, while for a maximally rotating Kerr black hole, $r_{\mathrm{ms}} = r_{\mathrm{g}}$. Thus, with increasing a r_{ms} moves closer to the BH, such that the resulting Fe Kα lines become broader since the velocity at r_{ms} increases. Furthermore, the importance of the gravitational redshift also increases with the diminishing of r_{ms}. As a result of both effects, the Fe Kα profile from rotating (Kerr) black holes is expected to have a stronger red tail and to be significantly broader than the profile seen from non-rotating Schwarzschild black holes (Fig. 1, right panel).
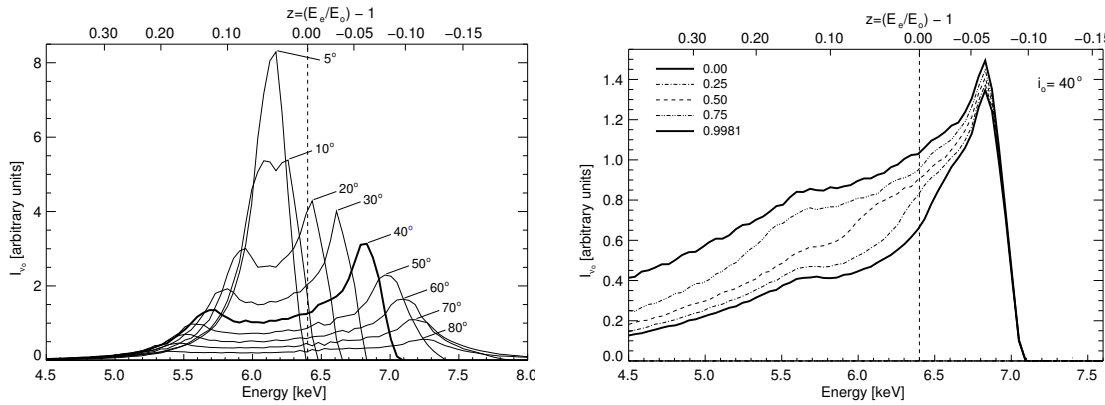
Fig. 1 Theoretical Fe Kα line profiles for a disk with a r^{-3} emissivity profile (after Wilms et al., 1998). Left: Line broadening as a function of the inclination angle. The profile at $i = 40°$ (thick lines) resembles the line profile seen in MCG−6-30-15 in the normal state. Right: Dependence of the line profile of the angular momentum for a Kerr BH, illustrating the increased strength of the red wing of the line with increasing angular momentum (after Wilms et al., 1998).

2.4 Emissivity Profile

As was shown in Sect. 2.2, the Fe Kα line is assumed to originate through fluorescence of hard photons irradiating the accretion disk. Since these hard photons were produced by Compton upscattering soft photons from the accretion disk in the ADC, the hard photon flux irradiating the accretion disk is in fact proportional to the soft photon flux emitted by the accretion disk. This luminosity profile depends on the details of accretion disk physics. In the most simplest of these models, the theory of Shakura & Sunyaev (1973), the disk emissivity is proportional to the local energy dissipation rate and scales as $\epsilon \propto r^{-3}$ away from the disk boundaries, thus justifying the choice for ϵ made in the previous section. In reality, accretion disks are most probably more complicated, and the general approach in the field has been to parameterize

$$\epsilon(r) \propto \begin{cases} r^{-\beta} & \text{for } r > r_{\text{ms}} \\ 0 & \text{for } r \leq r_{\text{ms}} \end{cases} \tag{1}$$

where r_{ms} is the marginally stable orbit, and where β is called the emissivity index (e.g., Laor, 1991). Figure 2 shows theoretical Fe Kα line profiles for a Schwarzschild black hole for $0 < \beta < 3$ and an inclination angle of 40°. As the line emissivity becomes more centrally concentrated with steeper emissivity profiles, i.e., larger β, the line profile becomes broader and can extend to well below 5 keV.

The results shown in the next sections have prompted several authors in recent years to modify the simple power law approach of Eq. 1. For example, Fabian et al. (2002) parameterize the emissivity profile outside r_{ms} by *two* power laws, while Reynolds et al. (2003b) also study Fe Kα line profiles for the relativistic accretion disks of Novikov & Thorne (1973) and Page & Thorne (1974), with a zero torque condition at r_{ms} and therefore reduced emissivity close to that radius. Furthermore, radiation emitted from the inner parts of the accretion disk can be focused back onto the accretion disk by the black hole (Cunningham, 1975). This "returning radiation" increases the Fe Kα luminosity from the inner parts of the accretion disk. Finally,
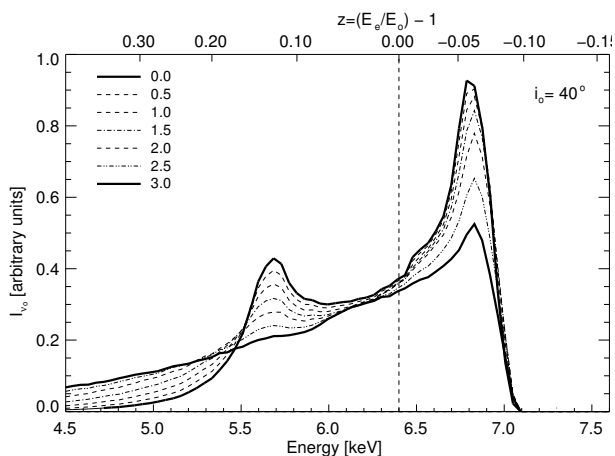
Fig. 2 Dependence of the Fe Kα line profile for power law emissitities $I \propto r^{-\beta}$ for a Schwarzschild BH and $i = 40°$ (after Wilms et al., 1998). For low β the Fe Kα profile is double humped.

line emission from within the marginally stable orbit could be important as well (Reynolds & Begelman, 1997).

3 RELATIVISTICALLY BROADENED FE Kα LINES IN AGN: MCG−6-30-15 AS A CASE STUDY

We will now turn to the observational evidence for the effects discussed in the previous section, concentrating on MCG−6-30-15, the prototype of an AGN with an extremely broad Fe Kα line.

In 1995, X-ray astronomy entered a new era with the first clear detection of a relativistically broadened Fe Kα line. In a long (∼4.5 d) *ASCA* observation of the nearby ($z = 0.008$) Seyfert galaxy MCG−6-30-15, Tanaka et al. (1995) found a clearly skew symmetric and possibly double humped line profile which was well described by the line profile expected from a Schwarzschild black hole (Fig. 3, left). This conclusion of a relativistically boadened Fe Kα line was confirmed in a later in-depth analysis of the time dependent X-ray spectrum. Here, Iwasawa et al. (1996) showed that the skew symmetric line profile seems to be the typical profile for 0.5–10 keV ASCA SIS-S0 count rates above ∼1 counts s^{-1}. During times of lower flux, however, in the so-called "deep minimum" state of MCG−6-30-15, the line profile is distinctly different (Fig. 3, right). Compared to the time averaged line profile, the "deep minimum" profile is significantly broader and cannot be explained with a line from a Schwarzschild black hole. This broad profile led Iwasawa et al. (1996) to deduce that there must be emission from within $6r_g$ and to argue that MCG−6-30-15 harbors a rotating black hole.

While the spectral resolution of the *ASCA* SIS was very well suited for studying the Fe Kα profile, its low sensitivity above the Fe K edge precluded a good measurement of the covering factor of the cold reflector. Since the strength of the reflection component increases with energy below 30 keV, the knowledge of $\Omega/2\pi$ is an important ingredient into the spectral modeling of the continuum. Later observations with *BeppoSAX* and *RXTE*, with their broadband coverage, allowed this determination, confirming the conclusions drawn from the *ASCA* data. These
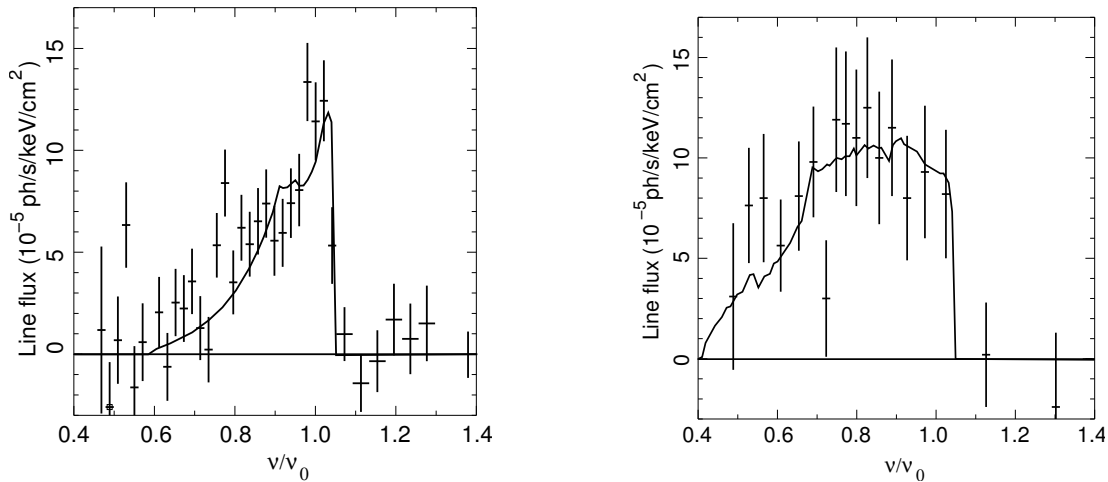
Fig. 3 Fe Kα profile of MCG−6-30-15 as determined by *ASCA*. Left: Time averaged profile. Right: Line profile measured during the "deep minimum state" (after Reynolds et al., 1997, Fig. 7). The continuum has been subtracted in both figures.

observations also resulted in a better understanding of the properties of the reflector and the broad band spectrum of MCG−6-30-15 (Guainazzi et al., 1999; Lee et al., 1998, 1999).

With the launch of the American *Chandra* and the European *XMM-Newton* in 1999, new powerful observational tools have become available. The LETGS and HETGS on *Chandra* allow very high spectral resolution studies of the 0.5–10 keV band with a moderate collecting area, while the Reflection Grating Spectrometer (RGS) and the three European Photon Imaging Cameras (EPIC) on *XMM-Newton* provide us with high resolution spectroscopy in 0.5–2 keV, and with X-ray CCD resolution from 0.5–10 keV, respectively, both with a very high throughput due to *XMM-Newton*'s large collecting area. Note that the high energy threshold of the EPIC cameras is high enough to provide us with at least a rough measure of $\Omega/2\pi$.

XMM-Newton observed MCG−6-30-15 on two occasions. During a 100 ksec observation in 2000 June, MCG−6-30-15 was found in low flux level ($F_{2-10} = 2.3 \times 10^{-11}$ erg s^{-1} cm^{-2}) similar to the ASCA "deep minimum" (Wilms et al., 2001; Reynolds et al., 2003b). The source was brighter in a later 315 ksec observation performed in 2001 July and August (Fabian et al., 2002; Fabian & Vaughan, 2003; Vaughan et al., 2003; Turner et al., 2003; Ballantyne et al., 2003). In the following, we will concentrate on the first *XMM-Newton* observation and for space reasons only briefly mention the results of the second longer *XMM-Newton* observation.

Figure 4 shows the X-ray lightcurve measured during the joint *XMM-Newton*/*RXTE* observation of 2000 June. The source is strongly variable down to timescales below 100 sec, as is typical for this source. Ignoring this complication, we will first analyze the time averaged X-ray spectrum and come back to the variability of the Fe Kα line below.

The left panel of Fig. 5 shows the result of fitting the *XMM-Newton* EPIC-pn data with a simple power law model. Spectra from single and double events, i.e., X-ray photons detected in one or two CCD pixels, respectively, are fitted simultaneously. As described in more detail by Wilms et al. (2001), deviations in the residuals for single and double events are an indication for pile up effects in the detector and serve as a check of our data extraction procedures. Note that the data shown for MCG−6-30-15 in Fig. 5 have not been rebinned further than what was
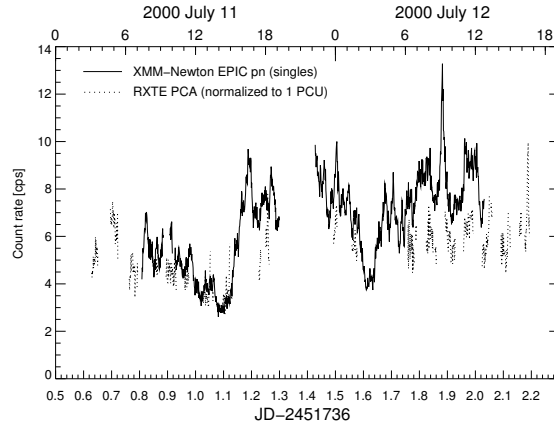
Fig. 4 Joint *XMM-Newton* (0.5–10 keV)/*RXTE* (3–15 keV) X-ray lightcurve of MCG−6-30-15 during the 2000 June observation.
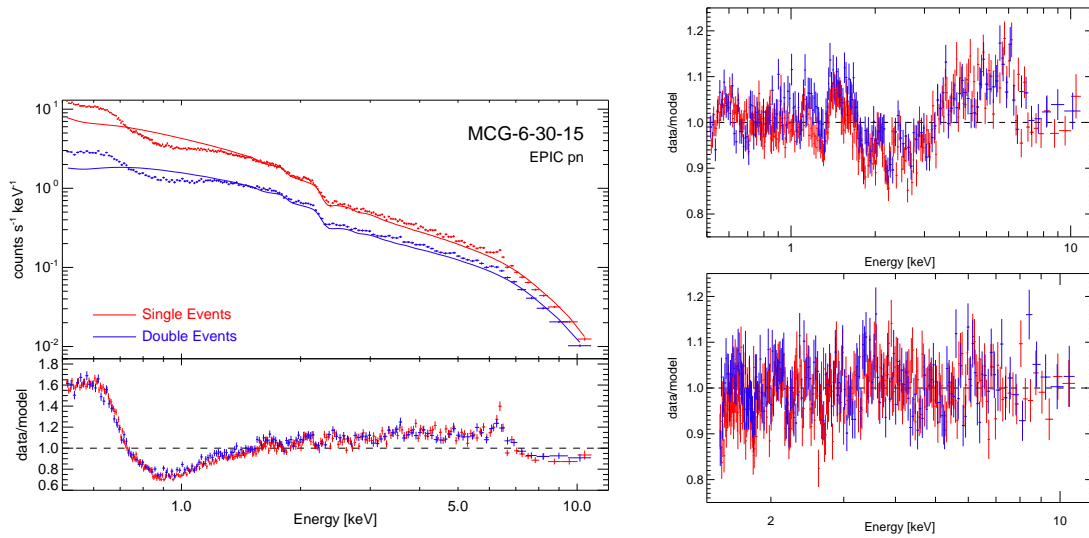
Fig. 5 Left: EPIC pn count rate spectrum and residuals for a simple power law fit to the data. Top right: Residuals (in terms of the ratio between the data and the predicted model flux) after modeling the low energy band with the empirical warm absorber model described in the text and with a narrow Fe Kα line. The broad lump in the residuals at energies above 4 keV is the broadened Fe Kα line. Bottom right: Residuals of the final fit which includes the relativistic line.

necessary to ensure the statistical significance of the χ^2 minimization procedure, such that all residuals will look rather "noisy" due to the large number of spectral bins in the Fe Kα band. Further rebinning would only result in nicer looking figures but not improve the statistical significance of the spectral features studied here.

As is obvious from Fig. 5, a power law does not describe the data well – there are clear deviations below ∼2 keV and a narrow feature at ∼6.4 keV. Furthermore, the continuum around

this narrow line, in which we expect to see the relativistically broadened Fe Kα line, is not well described by a power law. Before the Fe Kα regime is modeled, however, we first need to understand the low energy continuum. Earlier studies with *ASCA* had already shown (e.g., Reynolds, 1997; Reynolds et al., 1997) that the X-ray spectrum of MCG−6-30-15 below ∼2 keV is rather complex. The *ASCA* data were well described by a power law with two absorption edges due to ionized oxygen, which were attributed to a "warm absorber", i.e., ionized material in the vicinity of the black hole and known to be present in many Seyfert galaxies. With the availability of high resolution X-ray spectra from the *XMM-Newton* RGS and the *Chandra* HETGS, it is now possible to study this warm absorber in greater detail. Unfortunately, but perhaps not unexpectedly, these recent data pose more questions than they answer. Currently, there are two models explaining the soft X-ray spectrum: Lee et al. (2001), Turner et al. (2003), and Ballantyne et al. (2003) argue that the picture of a photoionized "warm absorber" is essentially correct and explain slight mismatches between predicted and observed absorption edge energies by invoking absorption in dust. At a very low level, the presence of relativistic emission lines from the accretion disk cannot be excluded (Turner et al., 2003). On the other hand, as first proposed by Branduardi-Raymont et al. (2001) and later extended by Sako et al. (2003), there are also models in which the soft X-ray continuum is explained by strong relativistic lines and in which the earlier *ASCA* results are misinterpretations due to its moderate spectral resolution.

Luckily enough, both models for the soft X-ray spectrum give equally good descriptions of the EPIC-pn spectrum (Wilms et al., 2001; Reynolds et al., 2003b), such that the interpretation of the X-ray continuum above 2 keV is not affected by the as of now unresolved conflict of the interpretation of the soft X-ray data. The top right panel of Fig. 5 shows the residuals from modeling the EPIC pn data with an empirical warm absorber model derived from the RGS. Again, a power law was used to model the continuum radiation, and the clear feature at 6.4 keV in the rest frame of MCG−6-30-15 is successfully described with a narrow Gaussian emission line. This latter spectral component with an equivalent width of ∼40 eV is most probably due to fluorescence radiation from cold material distant from the central black hole. Furthermore, we also add a relativistically smeared reflection continuum from a possibly ionized accretion disk, fixing the inclination of the disk to 30°. Clear residuals remain in the 3–8 keV band, which we interpret as a relativistic iron line. In our final fit, shown in the bottom right panel of Fig. 5, we therefore include a broad Fe Kα feature. This final model describes the data well (χ^2/dof = 1506/1312, see Fig. 6 for a νf_ν plot of the final spectral model). With $6.95^{+0}_{-0.15}$ keV the rest frame energy of the Fe Kα line is indicative of ionized iron, consistent with the assumed ionization of the reflecting accretion disk. The large width of the Fe Kα line results in a Fe Kα emissivity $I_{K\alpha}(r) \propto r^{-4.6\pm0.3}$, i.e., most of the line emission is found to originate very close to the black hole. This result is confirmed from the longer 315 ksec *XMM-Newton* observation analyzed by Fabian et al. (2002) and Fabian & Vaughan (2003), where the line emissivity is described by a broken power law with $I_{K\alpha}(r) \propto r^{-5.5\pm0.3}$ for $r < 6.1^{+0.8}_{-0.5} r_{\rm g}$ and $I_{K\alpha}(r) \propto r^{-2.7\pm0.1}$ outside this transition radius.

Before discussing the implications of this rather steep emissivity profile, it is important to discuss the limitations of the analysis outlined above. Obviously, the broad line parameters depend strongly on the assumed continuum model, which at first glance might seem to be rather "ad hoc". It is important, therefore, to study whether different approaches to the spectral modeling give essentially the same results or not. Here, we only give a short summary of the main results, see Reynolds et al. (2003b) for an extended discussion of these issues. First of all, we note that our study is based on the assumption that the spectral continuum is a pure power law. In principle, Comptonization spectra can be curved, thus mimicking broadened line features, however, applying realistic Comptonization models to the joint *XMM-Newton*/RXTE data leaves the Fe Kα parameters unchanged. Secondly, curvature could also be introduced
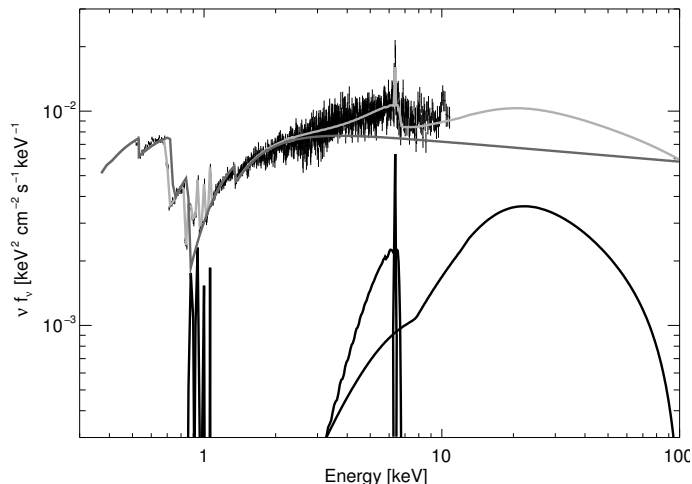
Fig. 6 Unfolded X-ray spectrum of MCG−6-30-15, showing the power-law continuum (dark grey), the spectral complexity below ∼2 keV, the narrow Fe Kα line, the relativistically broadened reflection continuum, and the relativistically broadened Fe Kα line. The light grey line is the total X-ray spectrum inferred from the data.

by the assumed reflection continuum. As of today, even the most advanced reflection (e.g., Nayakshin & Kallman, 2001; Ballantyne et al., 2002) most probably give only very simplified descriptions of the real reflection continua. Using different prescriptions for the reflection continuum, however, always results in similar Fe Kα profiles, leaving us with the impression that the Fe Kα parameters seem to be rather stable against the very different assumptions underlying the reflection continua. Thirdly, as shown by Fig. 4, the source is strongly variable on all timescales. Changes of the continuum photon index, Γ, with flux could in principle mimic a line broadening, and such a continuum variability is indeed present, as shown by the time variable hardness ratio of the source. The analysis of time dependent spectra shows, however, that while the Fe line *is* variable, $\beta > 3.5$ for the time dependent X-ray spectra as well (Reynolds et al., 2003b). Finally, it has recently been pointed out that partial covering models, in which the black hole is partially covered by absorbing material of high ($N_\mathrm{H} > 10^{21}\,\mathrm{cm}^{-2}$) column density, will result in curved continua and could thus mimic relativistic lines (e.g., Pounds, priv. comm.). Our *XMM-Newton* data from MCG−6-30-15 can indeed be described by such a model, without requiring a broadened line, however, when adding the RXTE data from >10 keV, there are strong deviations between the partial covering model and the observation. From all of these arguments we conclude that we have to consider the presence of a strongly broadened Fe Kα line in the data an observational reality. At the time of writing, this broadened line was the broadest seen in all Active Galactic Nuclei. Furthermore, the width of the line alone confirms the earlier conclusions of Iwasawa et al. (1996) that MCG−6-30-15 harbors a Kerr black hole, although our data are not good enough to constrain the angular momentum of the black hole.

As described in Sect. 2.4, in the accretion disk corona interpretation of Seyfert galaxies the inferred Fe Kα emissivity profile is mainly a measure of the local energy dissipation rate. Ignoring the effects of "returning radiation" for the moment, the inferred energy dissipation rate in the "deep minimum state" is $\propto r^{-4.6}$, or even steeper in the data of Fabian et al. (2002),

while the emissivity profile for a Shakura & Sunyaev (1973) accretion disk is $\propto r^{-3}$. Thus, the data imply that the energy dissipation close to the marginally stable orbit is higher than expected from theoretical models, suggesting the presence of an additional energy source close to the black hole.

What is the reason for this increased dissipation rate? First of all, we note that $\beta < 3.5$ for any accretion disk model. For example, as shown by Reynolds et al. (2003b) the inferred value of β is also too high when it is compared with that predicted for simple relativistic accretion disks such as those of Page & Thorne (1974). Furthermore, radial angular momentum transport in more realistic accretion disk models, where the viscosity is caused by the magnetorotational instability (MRI; Balbus & Hawley, 1998, and references therein), will result in an even smaller energy dissipation gradients.

One possible interpretation of the observational data is that the increased energy release is due to that of a magnetic couple between the region within the marginally stable orbit (e.g., the plunging region or the event horizon) and the accretion disk. Frame dragging effects such as those proposed by Agol & Krolik (2000) or Li (2002a,b,c) would allow to extract part of the rotational energy of the black hole and allow the energy dissipation in the accretion disk to increase. Such models have yet to be studied in detail, however, first results from describing the observations with Fe Kα profiles predicted from accretion disks torqued by a magnetic field at r_{ms} (Agol & Krolik, 2000) indicate that the observed line profiles could be explained by such models (Reynolds et al., 2003b, these fits also include the important effect of "returning radiation"). We note, however, that torquing the disk could suppress the formation of an accretion disk corona (Merloni & Fabian, 2003), such that more theoretical work is needed before a final conclusion can be drawn. As an example for such theoretical model we mention the recent work on line profiles from a geometry where the soft X-rays responsible for the fluorescence come from a point source above the rotational poles of the black holes, as expected, e.g., from the basis of a collimated outflow or jet (see also Ghisellini et al., 2004). As shown by Martocchia et al. (2002), the line profile of MCG−6-30-15 observed with *XMM-Newton* can in principle be reproduced in such a geometry. It is not yet clear, however, whether these alternative attempts are also able to reproduce the other observational features that led to the ADC picture of the continuum formation in Seyfert galaxies, and further work is clearly needed.

4 SUMMARY AND OUTLOOK

In this contribution we have discussed what we believe the current picture of the formation of the X-ray spectrum of Seyfert galaxies, Comptonization of soft photons close to a geometrically thin and optically thick accretion disk. We have shown that this picture naturally leads to the formation of a reflection hump and to the emission of a strong fluorescent Fe Kα line. Due to its vicinity to the supermassive black hole in the center of the AGN, the line emitting material is moving at relativistic speeds, resulting in a broadened Fe Kα line profile. We have shown that the line profile is affected by the local accretion disk efficiency, the black hole spin, and the inclination angle of the accretion disk with respect to the observer. The analysis of observations of relativistically broadened Fe Kα lines allows in principle to deduce these parameters from the line profile. We have shown how such an analysis proceeds, using 100 ksec of data from MCG−6-30-15 observed with *XMM-Newton*. These observations lead to very steep emissivity profiles. We speculate that such a concentration of the Fe Kα emissivity to close to the marginally stable orbit could be due to the extraction of energy from the black hole. We have also mentioned that special geometric setups for the soft photons (e.g., the "lamppost models") can in principle not yet excluded.

Due to these possibly important consequences, it is natural that MCG−6-30-15 is only one (albeit especially well studied) example of a whole class of sources. This had alread been realized

directly after the first discovery of the broad line in MCG−6-30-15, when systematic studies of *ASCA* data from Seyfert galaxies revealed complex Fe Kα profiles — then interpreted as relativistic broadened lines — in a majority of the observed sources (e.g., Nandra et al., 1997; Turner et al., 1997, and references therein). Higher signal to noise observations with *XMM-Newton* and *Chandra* still show the presence of such complex profiles in many AGN. Apart from MCG−6-30-15, we name, for example, the Seyfert galaxies MCG−5-23-16 (Dewangan et al., 2003) and Mrk 355 (Gondoin et al., 2002), or the quasar Q0056−363 (Porquet & Reeves, 2003). On the other hand, there are also sources in which no broadened component can be detected at all. Up to now, the best examples are perhaps NGC 4593 and NGC 5548, which can both be well modeled by pure power law continua with narrow Fe Kα lines from fluorescent material far away from the black hole and no evidence for a broadened line (Pounds et al., 2003; Reynolds et al., 2003a).

These exciting observational results indicate that there is no clear dependence between the class or luminosity of the observed object with the presence of a Fe Kα line, and that the real physical reason for what is responsible for the Fe Kα line profile is yet to be understood. One possible explanation could be that models for Compton reflection off moderately to highly ionized material result in strongly suppressed Fe Kα line strengths (e.g., Ballantyne et al., 2002, and references therein). Further observations with a higher signal to noise ratio which will be performed with *XMM-Newton* and *Chandra* in the near future, and with *Constellation-X* and *XEUS* will allow us to gain more insight into the physics of the line formation, and will allow us to study in even more detail the effects of strong gravity close to the black hole.

References

Agol E., Krolik J. H., 2000, ApJ, 528, 161

Balbus S. A., Hawley J. F., 1998, Rev. Mod. Phys., 70, 1

Ballantyne D. R., Ross R. R., Fabian A. C., 2002, MNRAS, 336, 867

Ballantyne D. R., Vaughan S., Fabian A. C., 2003, MNRAS, 342, 239

Ballantyne D. R., Weingartner J. C., Murray N., 2003, A&A, 409, 503

Basko M. M., 1978, ApJ, 223, 268

Branduardi-Raymont G., Sako M., Kahn S. M., Brinkman A. C., Kaastra J. S., Page M. J., 2001, A&A, 365, L140

Bromley B. C., Chen K., Miller W. A., 1997, ApJ, 475, 57

Cunningham C. T., 1975, ApJ, 202, 788

Dewangan G. C., Griffiths R. E., Schurch N. J., 2003, ApJ, 592, 52

Dove J. B., Wilms J., Maisack M. G., Begelman M. C., 1997, ApJ, 487, 759

Fabian A. C., Iwasawa K., Reynolds C. S., Young A. J., 2000, PASP, 112, 1145

Fabian A. C., Rees M. J., Stella L., White N., 1989, MNRAS, 238, 729

Fabian A. C., Vaughan S., 2003, MNRAS, 340, L28

Fabian A. C. et al., 2002, MNRAS, 335, L1

Fender R. P., 2001, MNRAS, 322, 31

Frank J., King A., Raine D., 1992, Accretion Power in Astrophysics, 2nd ed., Cambridge: Cambridge Univ. Press

Ghisellini G., Haardt F., Matt G., 2004, A&A, 413, 535

Gondoin P., Orr A., Lumb D., Santos-Lleo M., 2002, A&A, 388, 74

Guainazzi M. et al., 1999, A&A, 341, L27
Haardt F., 1997, Mem. Soc. Astron. Ital., 68, 73
Haardt F., Maraschi L., Ghisellini G., 1994o, ApJ, 432, L95
Iwasawa K. et al., 1996, MNRAS, 282, 1038
Laor A., 1991, ApJ, 376, 90
Lee J. C., Fabian A. C., Brandt W. N., Reynolds C. S., Iwasawa K., 1999, MNRAS, 310, 973
Lee J. C., Fabian A. C., Reynolds C. S., Iwasawa K., Brandt N., 1998, MNRAS, 300, 583
Lee J. C., Ogle P. M., Canizares C. R., et al., 2001, ApJ, 554, L13
Li L.-X., 2002a, ApJ, 567, 436
Li L.-X., 2002b, A&A, 392, 469
Li L.-X., 2002c, Phys. Rev. D, 65, 84047
Lightman A. P., White T. R., 1988, ApJ, 335, 57
Magdziarz P., Zdziarski A. A., 1995, MNRAS, 273, 837
Markoff S., Falcke H., Fender R., 2001, A&A, 372, L25
Markoff S., Nowak M., Corbel S., Fender R., Falcke H., 2003, A&A, 397, 645
Martocchia A., Matt G., Karas V., 2002, A&A, 383, L23
Martocchia A., Matt G., Karas V., Belloni T., Feroci M., 2002, A&A, 387, 215
Merloni A., Fabian A. C., 2003, MNRAS, 342, 951
Miller J. M., Fabian A. C., Wijnands, R., et al., 2002, ApJ 570, L69
Nandra K., George I. M., Mushotzky R. F., Turner T. J., Yaqoob T., 1997, ApJ, 477, 602
Nayakshin S., Kallman T. R., 2001, ApJ, 546, 406
Novikov I. D., Thorne K. S., 1973, In: C. DeWitt, B. DeWitt, eds., Black Holes — Les Astres Occlus.
    New York, London: Gordon and Breach, p. 345
Nowak M. A., Wilms J., Dove J. B., 2002, MNRAS, 332, 856
Page D. N., Thorne K. S., 1974, ApJ, 191, 499
Porquet D., Reeves J. N., 2003, A&A, 408, 119
Pounds K. A., Reeves J. N., Page K. L., Edelson R., Matt G., Perola G. C., 2003, MNRAS, 341, 953
Reynolds C. S., 1997, MNRAS, 286, 513
Reynolds C. S., Begelman M. C., 1997, ApJ, 487, 109
Reynolds C. S., Brenneman L. W., Wilms J., Kaiser M. E., 2003a, MNRAS, submitted
Reynolds C. S., Nowak M. A., 2003, Phys. Rep., 377, 389
Reynolds C. S., Ward M. J., Fabian A. C., Celotti A., 1997, MNRAS, 291, 403
Reynolds C. S., Wilms J., Begelman M. C., Kendziorra E., Staubert R., 2003b, MNRAS, in press
Sako M., Kahn, S. M., Branduardi-Raymont, G., et al., 2003, ApJ, 596, 114
Shakura N. I., Sunyaev R., 1973, A&A, 24, 337
Speith R., Riffert H., Ruder H., 1995, Comput. Phys. Commun., 88, 109
Stern B. E., Poutanen J., Svensson R., Sikora M., Begelman M. C., 1995, ApJ, L13
Tanaka Y. et al., 1995, Nature, 375, 659
Thorne K. S., 1974, ApJ, 191, 507
Turner A. K., Fabian A. C., Vaughan S., Lee J. C., 2003, MNRAS, 346, 833
Turner T. J., George I. M., Nandra K., Mushotzky R. F., 1997, ApJS, 113, 23
Vaughan S., Fabian A. C., Nandra K., 2003, MNRAS, 339, 1237
White T. R., Lightman A. P., Zdziarski A. A., 1988, ApJ, 331, 939
Wilms J., Reynolds C. S., Begelman M. C., Reeves J., Molendi S., Staubert R., Kendziorra E., 2001,
    MNRAS, 328, L27
Wilms J., Speith R., Reynolds C. S., 1998, In: F. W. Hehl, C. Kiefer, R. Metzler, ed, Black Holes:
    Theory and Observation, Lecture Notes in Physics No. 514. Berlin, Heidelberg: Springer, p. 69
Zdziarski A. A., Lubiński P., Smith D. A., 1999, MNRAS, 303, L11
Zdziarski A. A., Poutanen J., Mikołajewska J., Gierliński M., Ebisawa K., Johnson W. N., 1998,
    MNRAS, 301, 435